Journal of Power Sources 195 (2010) 4272–4277

Contents lists available at ScienceDirect

Journal of Power Sources

journal homepage: www.elsevier.com/locate/jpowsour

Composite nonwoven separator for lithium-ion battery: Development and characterization

Tae-Hyung Cho[a,*], Masanao Tanaka[a], Hiroshi Ohnishi[a], Yuka Kondo[a], Miyata Yoshikazu[a], Tatsuo Nakamura[a], Tetsuo Sakai[b,**]

[a] Japan Vilene Co., Ltd, 7 Kita-Tone, Koga, Ibaraki 306-0213, Japan
[b] National Institute of Advanced Industrial Science and Technology, Kansai, 1-8-31 Midorigaoka, Ikeda, Osaka 563-8577, Japan

ARTICLE INFO

Article history:
Received 23 October 2009
Received in revised form 5 January 2010
Accepted 8 January 2010
Available online 18 January 2010

Keywords:
Li-ion battery
Nonwoven separator
Polyolefin nonwoven
Nano-fiber nonwoven
Ceramic composite separator

ABSTRACT

A new type composite nonwoven separator has been developed by combining a polyacrylonitrile (PAN) nano-fiber nonwoven and ceramic containing polyolefin nonwoven. The physical, electrochemical and thermal properties of the separator were investigated. The separator has mean pore size of about 0.8 μm as well as narrow pore-size distribution. Besides, the separator possesses higher porosity and air permeability than a conventional microporous membrane separator. The separator showed tensile strength of 46 N 5 cm^{-1} at 10% elongation. Any internal short circuit was not observed for cells with the separator during charge–discharge test, and the cells showed stable cycling performance. Moreover, the cells showed better rate capabilities than cells with the conventional one. On a hot oven test at 150 °C, the composite nonwoven separator showed better thermal stability than the conventional one. In addition, internal short circuit by thermal shrinkage of separator was not observed for a cell with the separator at 150 °C for 1 h.

1. Introduction

The market shares of the lithium-ion battery for the civilian applications, such as notebook computer, cellular phone, digital camera and camcorder, have been increased year by year. In addition, a large scale lithium-ion battery has been studied intensively to expand its current usage, power sources for portable electric devices, into industrial usage, such as power sources for plug in electric vehicles (PEVs), hybrid vehicles (HEVs), power tools and robots. The industrial application demands more energy and power density from the battery as well as safety concerns [1–3].

A nonwoven fabric is very attractive material to satisfy the demands, because it has high porosity [4] and can readily composite with other materials such as ceramic powder [5–7] and polymer electrolyte [8–12]. The former can enhance power density of the battery and the latter can provide extra function such as high thermal stability to the battery. As a matter of fact, we had developed two types of nonwoven separators with close thickness and pore size to a conventional microporous membrane separator [7,13,14]. The one is a nano-fiber nonwoven separator. Cells with the separator showed outstanding rate capabilities and stable cycling performances. However, it suffers from low tensile strength and thermal stability above 150 °C in an electrolyte. The other is a ceramic composite nonwoven separator. Cells with the separator could provide stable battery performances and better thermal stabilities than a cell with a conventional microporous membrane separator. But, it also has some drawbacks for instance dropping out of ceramic particles and low air permeability due to the large amount of ceramic powder inside the separator. In order to increase the air permeability of the separator, the amount of the ceramic powder has to be reduced, but it leads large pore size and inhomogeneous pore-size distribution resulting internal short circuit during charge–discharge process. Therefore, it is necessary to remove these drawbacks of the nonwoven separators to apply them for practical use.

Recently, we have developed a new type composite nonwoven separator by combining nano-fiber nonwoven and ceramic containing nonwoven in order to remove the shortcomings of the formerly developed separators. The ceramic containing polyolefin nonwoven part could provide high tensile strength and thermal stability to the separator and nano-fiber nonwoven part prevents dropping out of the ceramic powder as well as furnishing small pore-size and narrow pore-size distributions to the separator. Therefore, in this paper, we would report physical and electrochemical properties of the composite nonwoven separator.

* Corresponding author at: Japan Vilene Co., Ltd, Research and Development Center, 7 Kitatone, Koga, Ibaraki 306-0213, Japan. Tel.: +81 280 92 7276; fax: +81 280 92 7273.
** Corresponding author. Fax: +81 72 751 9623.
E-mail addresses: th-cho@vilene.co.jp (T.-H. Cho), sakai-tetsuo@aist.go.jp (T. Sakai).

0378-7753/$ – see front matter © 2010 Elsevier B.V. All rights reserved.
doi:10.1016/j.jpowsour.2010.01.018

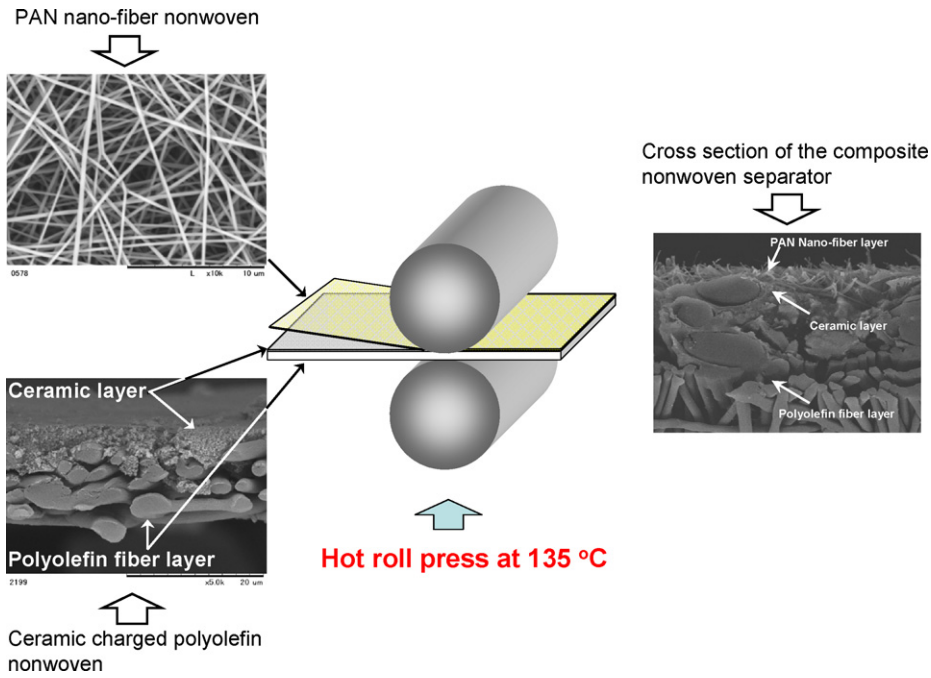

Fig. 1. Schematic depiction of combining process.

2. Experimental

2.1. Fabrication of the composite nonwoven separator

A polyolefin nonwoven for filling ceramic powder was fabricated by a two step wet laid method. An aqueous suspension was prepared by dispersing polyethylene (PE)–polypropylene (PP) sheath core composite fibers, which consists of 50 wt.% of PE sheath part and 50 wt.% of PP core part, with fineness of 0.8 dtex (10 μm in diameter) and length of 5 mm in distilled water, and then it was laid down on a screen web to form a fiber web. The fiber web was heat bonded by using a hot roll press at 135 °C. After that, another aqueous suspension was prepared by using fine PP fibers with fineness of 0.02 dtex (2 μm in diameter) and 2 mm in length, and then it was laid down on the previously prepared nonwoven, and then the web was heat bonded again by the hot roll press at 135 °C.

A PAN nano-fiber nonwoven was prepared by an electrospinning technique. The spinning conditions of the PAN nano-fiber nonwoven were described in the previous report [13].

Prior to combine the base nonwoven with the PAN nano-fiber nonwoven, we filled silica or alumina powder with mean particle size of 0.2 μm by spraying the powder on the one side of the base nonwoven. And then, the PAN nano-fiber nonwoven and the ceramic charged nonwoven were combined through the hot roll press at 135 °C. A scheme for the combining process was given in Fig. 1.

2.2. Physical and electrochemical characterizations

The morphologies of the composite nonwoven separator were observed by scanning electron microscope (Miniscope TM-1000, Hitachi, Japan).

The mean pore size and pore-size distributions of the composite nonwoven separators and the base nonwoven were measured by bubble point method using Automated Perm Porometer (Porous Materials, Inc., USA). The Gurley values of the separators were measured in accordance with Japanese industrial standard JIS P8177 using Gurley type densometer (Yasuda Co., Japan). The tensile strengths of the separators were measured at strain rate of $5 \times 10^{-2}\ s^{-1}$ using UCT-100 (Orientec Co., Japan). The samples were cut into 200 mm × 50 mm (length and width) and then carefully mounted with a gauge length of 100 mm.

Battery tests such as cycle life and rate capability were carried out in the voltage range of 3.0–4.2 V at 20 °C using 2032 coin type cell consisting of $LiCoO_2$ electrode as a cathode, graphite electrode purchased from Hohsen Co. Ltd. as an anode and 1 M $LiPF_6$-EC/DEC (1:1 in volume) (Kishida Chemical Co., Ltd.) as an electrolyte. The reversible capacities of the both electrodes were about 1.7 mAh cm^{-2} and the anode to the cathode capacity ratio of fabricated cells was about 1.15. The cathode for the coin type cells was fabricated as follow; the lithium cobalt oxide (Nippon Chemical industrial Co. Ltd., Japan), ketjen black and polyvinylidenefluoride (90:5:5 in wt.%) were blended in N-methyl-

Table 1
Physical properties of separators.

Properties	Unit	CNS No. 1	CNS No. 2	Celgard® 2400
Composition	–	Polyolefin, PAN, SiO_2	Polyolefin, PAN, Al_2O_3	Polypropylene
Weight of separator	g m^{-2}	20	19	14.3
Ceramic	%	15	11	–
Weight ratio of PAN		12	13	–
Thickness	μm	34	33	25
Mean pore size	μm	0.86	0.79	<0.1
Porosity	%	46	50	40
The Gurley value	s 100 cm^{-3}	1.3	1.2	730

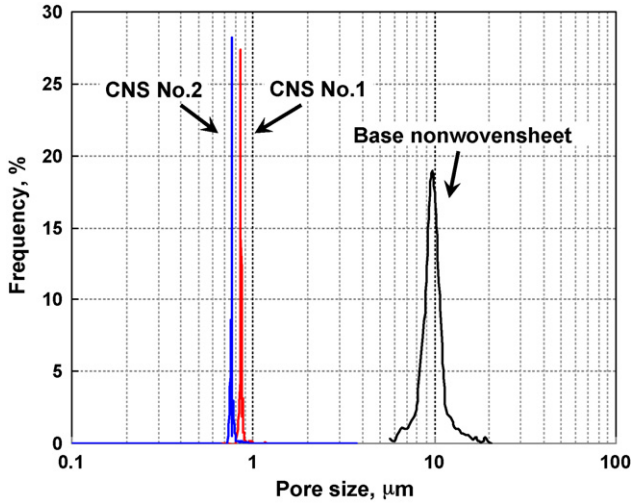

Fig. 2. Pore-size distributions of the base nonwoven sheet, the CNS No. 1 and No. 2.

2-pyrrolidinon. The blended slurry was coated on an aluminum foil, and then dried at 120 °C. The cathode sheet was roll-pressed and then punched out as disks from the sheet with 12 mm in diameter. The electrodes, cathode and anode, and separators were dried at 140 °C for 6 h and 90 °C for 1 day under vacuum state, respectively. The cells were assembled in a glove box under Ar atmosphere.

3. Results and discussion

Small pore-size and narrow pore-size distribution are generally requisite properties to a separator for the lithium-ion battery. Because wide pore-size distribution leads inhomogeneous current distribution resulting poor cycle life of battery and dendritic growth of lithium. In our previous work [7], we had tried to control pore size and pore-size distribution of a nonwoven by filling of ceramic powder. Since the pore size and the pore-size distribution can be controlled by volume of the ceramic powder, large amount of the ceramic powder (more than 30 wt.% to total weight of separator) has to be inside of the separator in order to obtain small pore-size and narrow pore-size distribution. Accordingly, it is inevitable increasing Gurley value of the separator. As a result, we found that the Gurley value of the separator has to be more than 200 s 100 cm^{-3} to obtain stable battery performance. However, since the pore size and the pore-size distribution of the composite nonwoven separator are controlled by not only quantity of the ceramic powder but also PAN nano-fiber nonwoven, the separator does not need large volume of the ceramic powder. Consequently, it is possible to manufacture a separator having small pore-size and narrow pore-size distribution without considerable loss on the air permeability. Fig. 2 shows pore-size distributions of the base nonwoven, the composite nonwoven separators containing silica and alumina powder measured by the bubble point method. Hereinafter, we refer the silica charged composite nonwoven separator as CNS No. 1 and the alumina charged nonwoven separator as CNS No. 2. The base nonwoven fabric showed mean pore size of about 10 μm and wide pore-size distribution. The large mean pore size of the nonwoven fabric reduced and its pore-size distribution became narrow by charging the ceramic powders and combining with PAN nano-fiber nonwoven fabric. The CNS No. 1 and No. 2 shows mean pore size of 0.86 μm and 0.79 μm, respectively. The brief physical properties of the CNS No. 1, No. 2 and the Celgard membrane were summarized in Table 1.

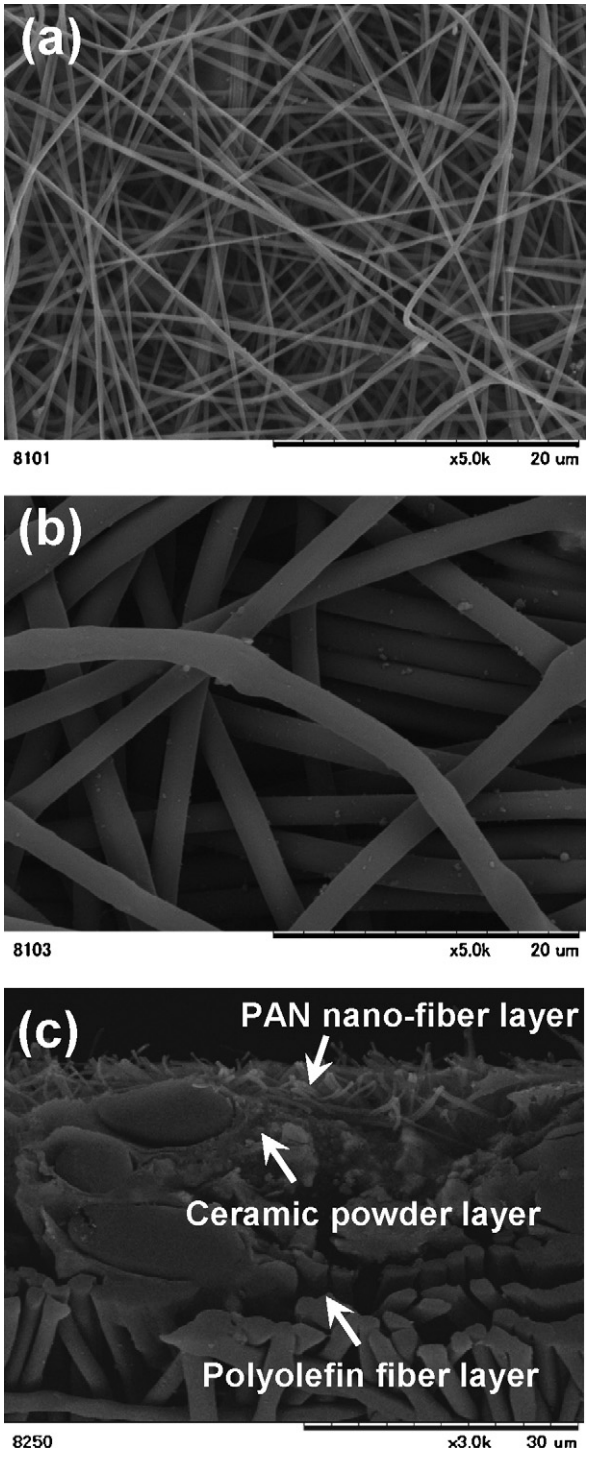

Fig. 3. SEM photographs for the CNS No. 1; (a) PAN nano-fiber nonwoven side, (b) polyolefin nonwoven side and (c) cross-section of the separator.

Fig. 3(a)–(c) shows surface of the PAN nano-fiber nonwoven layer, polyolefin nonwoven layer and cross-section of the CNS No. 1, respectively. The ceramic powder was sandwiched by the PAN nano-fiber nonwoven and the polyolefin nonwoven layer, and the ceramic particles were not observed on the surface of the CNS as shown in Fig. 3. In order to confirm dropping out of the powder from the separator, we roughly crumpled the separator by hand and then measured the weight loss of the separator. Despite of binder free, negligible weight loss (less than 1%) was observed from the separator after the crumpling. This result indicates that the structure of

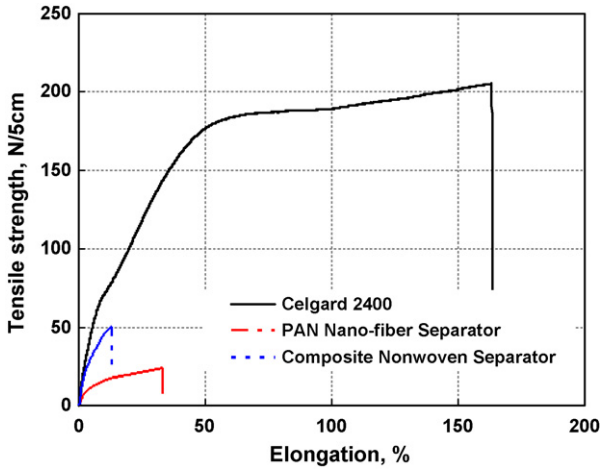

Fig. 4. Stress–strain curves for the Celgard® 2400, the PAN nano-fiber nonwoven and the CNS No. 1.

the separator is very suitable for preventing drop out of the ceramic powder from the separator.

Fig. 4 shows tensile strength–elongation curves for the Celgard membrane, the PAN nano-fiber nonwoven separator with thickness of 35 μm and the CNS. The obtained properties were summarized in Table 2. Since the Celgard membrane was prepared by stretching a polyolefin film along to the machine direction, it showed very high tensile strength to the machine direction. The obtained tensile strength of the separator at 2, 5 and 10% elongation were 23, 46, 70 N 5 cm^{-1}, respectively. Despite of their similar thickness, the two nonwoven separator showed different tensile strengths. The PAN nano-fiber nonwoven showed the lowest tensile strength of 7, 12 and 16 N 5 cm^{-1} at 2, 5 and 10% elongation. The CNS showed higher tensile strength than that of the PAN one. The measured tensile strengths of the CNS at the same elongation were 18, 31 and 46 N 5 cm^{-1}. The difference in the tensile strength between the PAN nano-fiber nonwoven and the CNS can be attributed to their composition. The PAN one consists of only PAN nano-fiber, thus it does not has any binder inside of it. On the contrary, the CNS contains thermally bondable fibers (polyolefin sheath core composite fiber, 0.8 dtex). Although the CNS has low tensile strength compared to the Celgard membrane, we believe that the separator can stand for deformation during winding process.

Battery performances for cells with the Celgard membrane, the CNS No. 1 and No. 2 were investigated. At the first cycle, the cells were charged up to 4.2 V under constant current–constant voltage mode, and then discharged to 3.0 V under constant current mode. The initial 10 charge–discharge cycles were tested with a 0.2 C-rate. Following charge–discharge tests were carried out with a 0.5 C-rate. Fig. 5(a) and (b) shows charge–discharge curves at the 0.2 C-rate and capacity retention ratios as a function of cycle number of the test cells, respectively. All of the cells showed similar coulombic efficiencies of about 90% at the first cycle. Any unstable voltage profiles were not observed for the cells with the CNSs as shown in Fig. 5(a) despite of their low Gurley values. The stable voltage profiles would be ascribed to the small pore-size and narrow pore-size distribution of them. The cells with the CNS No. 1 and No. 2 showed stable cycling performances through the charge–discharge tests with capacity retention ratios of 86.0 and 88.5% covering 200 cycles, respectively.

Table 2
The tensile properties of the separators.

Elongation	Unit	PAN nonwoven	CNS No. 1	Celgard® 2400
2%	N 5cm^{-1}	7	18	23
5%		12	31	46
10%		16	46	70
Break down		24	50	204

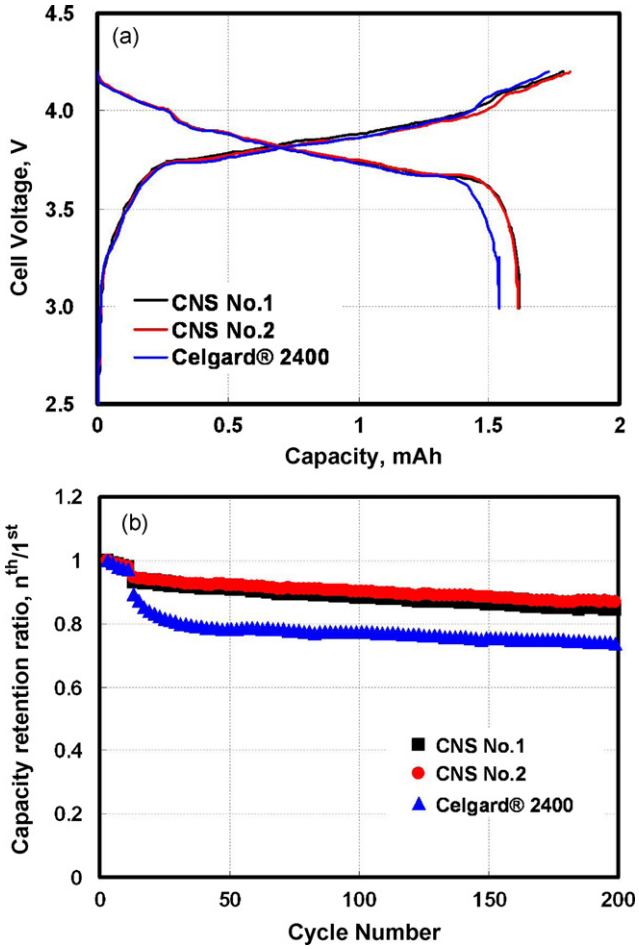

Fig. 5. (a) Initial charge–discharge curves for the cells with the Celgard® 2400, the CNS No. 1 and No. 2. (b) Discharge capacities vs. cycle numbers of the test cells.

Fig. 6 shows rate capabilities of cells with the separators. The rate capabilities of the cells were investigated as follow; the test cells were charged up to 4.2 V at the 0.2 C-rate, and then discharged to 3.0 V at the C-rates of 0.2, 0.5, 1, 2, 4 and 8 C. The obtained

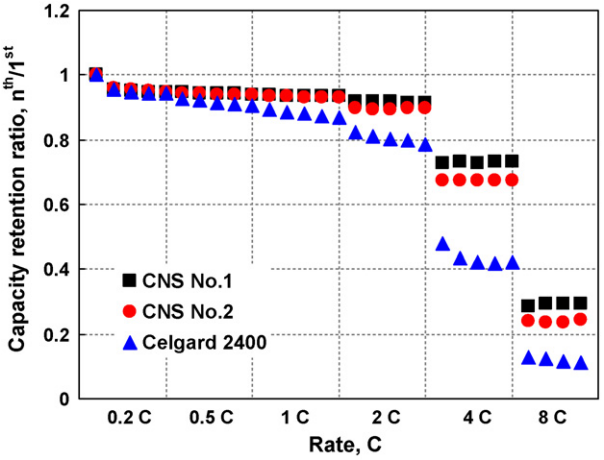

Fig. 6. Results of rate capability tests for the cells with the Celgard® 2400, the CNS No. 1 and No. 2.

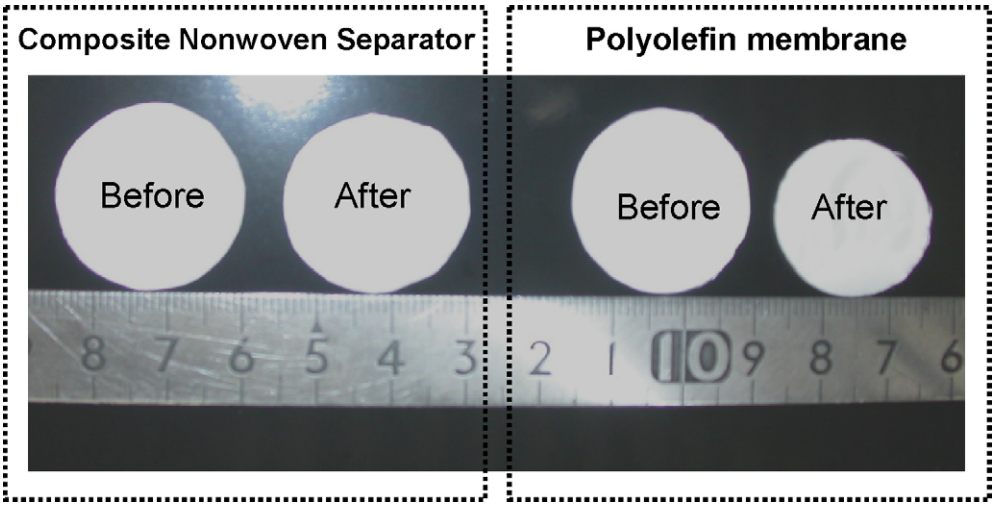

Fig. 7. Photographs of the CNS No. 1 and a conventional microporous membrane before and after hot oven test at 150 °C for 10 min.

discharge capacity of the cell with the Celgard membrane was gradually decreased with increase in the C-rate up to the 2 C-rate, and then abruptly decreased with increasing the C-rate up to 8 C-rate. The capacity retention ratios at the 4 and 8 C-rate were 42 and 11%, respectively. The cells with the CNSs showed better rate capabilities than the cells with the Celgard one. The obtained discharge capacities of the cells with the CNSs at 2, 4, and 8 C-rate were about 90, 70 and 27% of the initial discharge capacities. The better rate capabilities of the cells with the CNSs can be ascribed to their high porosities and low Gurley values than that of the Celgard one.

In order to investigate thermal stabilities of separators, a hot oven test was conducted for a polyolefin membrane and the CNS No. 1 at 150 °C for 10 min under air atmosphere. The results were presented in Fig. 7. After the hot oven test, the polyolefin membrane showed thermal shrinkage of about 20% in diameter (36% in area). On the contrary, The CNS No. 1 showed only about 4% of thermal shrinkage in diameter (8% in area). Subsequently, hot oven tests using CR-2032 coin type cells, which were charged up to 4.2 V, with the Celgard membrane, the PAN nano-fiber nonwoven separator and the CNS No. 1 were carried out by exposing the cells at 150 °C for 1 h. During the hot oven test, variations for open circuit voltage of the cells were monitored. Results of the hot oven tests were given in Fig. 8. The cells with the Celgard and the PAN nano-fiber nonwoven separator showed sudden voltage drop after 10 and 14 min from the start of the test, respectively, probably due to the internal short circuit by shrinking of the separators. On the other hand, the cell with the CNS No. 1 showed gentle voltage drop and any sudden voltage change was not observed during the hot oven test. The results indicate that the CNS is thermally stable at high temperature of 150 °C in the liquid electrolyte.

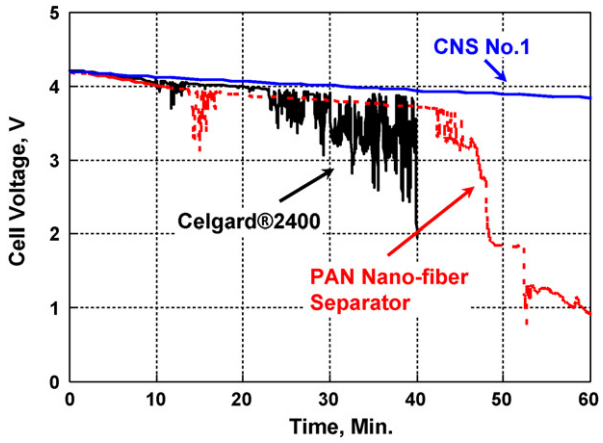

Fig. 8. The open circuit voltage profiles for the cells with the Celgard® 2400, the PAN nano-fiber nonwoven and the CNS No. 1 during the hot oven test at 150 °C for 1 h.

4. Conclusions

In order to enhance physical and electrochemical properties of the nonwoven separators, we have tried to develop a new type composite nonwoven separator by combining ceramic containing polyolefin nonwoven and PAN nano-fiber nonwoven. By combining the two nonwovens, we could successfully develop a separator having small pore-size and narrow pore-size distribution as well as high air permeability. The combination of PAN and polyolefin nonwoven separators retained the ceramic powder better in the composite nonwoven separator. Unstable voltage profile caused by internal short circuit was not observed during charge–discharge tests for cells with the CNSs and the cells showed stable cycling performance with high capacity retentions of about 88% covering 200 cycles. The cells with the CNSs showed better rate capabilities than that with the Celgard membrane by help of their high air permeability and porosity. The CNSs showed thermal shrinkage of about 4% at 150 °C under air atmosphere, and a cell with the separator did not showed any internal short circuit caused by thermal shrinkage of separator even though it was exposed at 150 °C for 1 h. Therefore, the newly developed composite nonwoven separator can be a promising candidate for separators of the lithium-ion battery.

References

[1] M.S. Whittingham, Chem. Rev. 104 (2004) 4271.
[2] M.S. Wu, P.C.J. Chiang, Electrochim. Acta 52 (2007) 3719.
[3] Y.B. He, Q. Liu, Z.Y. Tang, Y.H. Chen, Q.S. Song, Electrochim. Acta 52 (2007) 3534.
[4] P. Kritzer, J.A. Cook, Electrochem. Soc. 154 (2007) A481.
[5] S. Augustin, V.D. Hennige, G. Hörpel, C. Hying, P. Haug, A. Perner, M. Pompetzki, T. Wöhrle, C. Wurm, D. Ilic, Meet. Abstr.-Electrochem. Soc. 502 (2006) 84.
[6] S. Augustin, V. Hennige, G. Hoerpel, C. Hying, M. Saito, Meet. Abstr.-Electrochem. Soc. 502 (2006) 89.
[7] T.-H. Cho, M. Tanaka, H. Onishi, Y. Kondo, T. Nakamura, H. Yamazaki, S. Tanase, T. Sakai, Electrochem. Soc. 155 (2008) A699.

[8] S.-S. Choi, Y.S. Lee, C.W. Joo, S.G. Lee, J.K. Park, K.-S. Han, Electrochim. Acta 50 (2004) 339.
[9] Y.M. Lee, J.-W. Kim, N.-S. Choi, J.A. Lee, W.-H. Seol, J.-K. Park, J. Power Sources 139 (2005) 235.
[10] K. Gao, X. Hu, C. Dai, T. Yi, Mater. Sci. Eng. B 131 (2006) 100.
[11] P. Kritzer, J. Power Sources 161 (2006) 1335.
[12] D. Bansal, B. Meyer, M. Salomon, J. Power Sources 178 (2008) 848.
[13] T.-H. Cho, T. Sakai, S. Tanase, K. Kimura, Y. Kondo, T. Tarao, M. Tanaka, Electrochem. Solid-state Lett. 10 (2007) A159.
[14] T.-H. Cho, M. Tanaka, H. Onishi, Y. Kondo, T. Nakamura, H. Yamazaki, S. Tanase, T. Sakai, J. Power Sources 181 (2008) 155.